

POLYNOMIAL CHAOS EXPANSIONS FOR STIFF RANDOM ODEs*

WENJIE SHI[†] AND DANIEL M. TARTAKOVSKY[‡]

Abstract. Generalized polynomial chaos (gPC), often combined with mono-implicit Runge–Kutta (MIRK) methods, is widely used to solve random ODEs. We investigate the impact of stiffness of random ODEs on the gPC performance. We start by extending pragmatic definitions of stiffness used in deterministic ODEs to their random counterparts. Then we introduce gPC with parallel MIRK schemes to solve random stiff ODEs, in which a suitable parallelism partially alleviates the curse of dimensionality. Our stiffness analysis comprises two parts: (i) the relationship between Jacobians of random ODEs and the corresponding gPC equations and (ii) stiffness of the gPC equations. It provides a direct way to determine whether a random ODE and/or the corresponding gPC equations are stiff. This theoretical analysis plays a key role in designing numerical implementations not only of gPC but also of other methods of stochastic computation, e.g., Monte Carlo simulations and stochastic collocation. A series of computational experiments is used to demonstrate the agreement between our theoretical analysis and numerical results and to establish gPC with parallel MIRK as a feasible and effective tool for solving stiff random ODEs.

Key words. stiff equations, gPC, parallel mono-implicit Runge–Kutta, random ODE

MSC codes. 65C20, 65C30, 60H35

DOI. 10.1137/21M1432545

1. Introduction. Stiff equations play an important role in various fields of science and engineering. Stiffness can render explicit methods for solving differential equations unworkable [10, 19] and undermine the accuracy of forward integration [19, 30]. Even classic implicit Runge–Kutta methods (IRKs), possessing high efficiency and stability, encounter reduction in the order of accuracy; e.g., an A-stable IRK can produce highly unstable solutions, and its solution accuracy does not match the order of a method used [6, 14, 15, 19, 28]. The numerical treatment of stiff equations engendered such concepts as A-stability [11], $A(\alpha)$ -stability [40], A_0 -stability [9], L-stability [12], and B-convergence [14, 15, 19]. When quantified probabilistically, inevitable uncertainty in parameterizations of stiff problems gives rise to stiff random equations. To the best of our knowledge, theoretical analyses of stiff random ODEs or PDEs are scarce.

Our study deals with stiff random ODEs,

$$(1.1a) \quad \frac{d\mathbf{x}}{dt}(t, \omega) = \mathbf{f}(t, \boldsymbol{\xi}(\omega), \mathbf{x}(t, \omega)), \quad t \in (0, T], \quad \omega \in \Omega,$$

subject to an initial condition

$$(1.1b) \quad \mathbf{x}(0, \omega) = \boldsymbol{\varphi}(\boldsymbol{\xi}(\omega)), \quad \omega \in \Omega.$$

*Submitted to the journal’s Methods and Algorithms for Scientific Computing section July 9, 2021; accepted for publication (in revised form) November 29, 2021; published electronically May 2, 2022.

<https://doi.org/10.1137/21M1432545>

Funding: The work of the first author was supported by the Department of Education of Hubei Province under grant B2017062.

[†]School of Mathematical and Physical Sciences, Wuhan Textile University, Wuhan 430073, People’s Republic of China (wenjieshihust@gmail.com).

[‡]Energy Resources Engineering, Stanford University, Stanford, CA 94305 USA (tartakovsky@stanford.edu).

This problem is parameterized by a set of N random coefficients $\boldsymbol{\xi}(\omega) \triangleq (\xi_1(\omega), \xi_2(\omega), \dots, \xi_N(\omega))$ defined on a complete probability space $(\Omega, \mathcal{F}, \mathbb{P})$, with the sample space Ω , the σ -algebra $\mathcal{F} \subset 2^\Omega$, and the probability measure \mathbb{P} . The deterministic functions $\mathbf{f} \in \mathbb{R}^d$ and $\boldsymbol{\varphi} \in \mathbb{R}^d$ are such that the solution, $\mathbf{x}(t, \omega) \in \mathbb{R}^d$, exists almost surely for any realization of the parameters $\boldsymbol{\xi}(\omega)$. The paucity of literature on the stiffness of random ODEs is such that the very definition of stiffness of (1.1) appears to be absent. Nevertheless, numerical solutions of (1.1) are routinely obtained with Monte Carlo methods [13], the method of distributions [24, 39], generalized polynomial chaos (gPC) [17, 32, 33, 34, 41], stochastic collocation [3, 4, 27, 34, 42], etc.

These and other techniques for stochastic computation have to contend with two interconnected challenges. The first is often referred to as “long-time integration problem” and stems from an empirical observation that the structure of the randomness becomes more complex as time increases. It can be ameliorated by, e.g., dynamic modification of the gPC basis [16, 26]. The second challenge is due to the presence of realizations of the random parameter set $\boldsymbol{\xi}(\omega)$, for which some state variables $x_i(t)$ have much faster dynamics than others. The resulting stiffness has been tackled by, e.g., introducing artificial “time-stretching” to align realizations of random trajectories [2, 5, 23] rather than by deploying specialized stiff solvers such as mono-implicit Runge–Kutta (MIRK) schemes [6, 8, 38].

The gPC method is attractive because of its fast (often exponential) convergence rate [17, 32, 33, 34, 41]. At the same time, gPC suffers from the curse of dimensionality; i.e., its computational cost increases dramatically with the number of underlying random variables, N [34, 41]. It stands to reason that possible stiffness of (1.1) affects these key features of gPC. Specifically, the stiffness of (1.1) is expected to translate into the stiffness of a system of ODEs for the coefficients of a gPC expansion (aka gPC equations), an issue that remains largely unexplored. Likewise, the stiffness of (1.1) might affect the performance of numerical strategies developed to tackle the curse of dimensionality [3, 27, 34, 41, 42]. A goal of this study is to address these issues in a systematic way that facilitates the design of efficient parallelizable gPC algorithms for stiff random ODEs. Other numerical techniques of stochastic computation, such as Monte Carlo simulations and stochastic collocation, also benefit from this analysis.

In section 2, we extend some pragmatic definitions of stiffness of deterministic ODEs to the random case. Section 3 contains a description of our strategy to solve stiff random ODEs like (1.1), in which the gPC equations are solved with a parallel MIRK scheme. Our theoretical analysis, presented in section 4, consists of two parts. The first relies on our definition of stiff random ODEs to determine whether (1.1) is stiff. The second part relies on the Jacobian matrices of a linearized version of (1.1) used to construct the gPC equations to determine whether the latter are stiff. In section 5, we demonstrate our theoretical analysis on several ODEs in the form of (1.1). These examples also highlight the effectiveness of the gPC with parallel MIRK method. Major conclusions drawn from our study are summarized in section 6.

2. Definitions of stiffness. A practical way to identify the stiffness of an ODE is to compare the costs of obtaining its solution with stiff and nonstiff ODE solvers. A mathematically rigorous definition of stiffness is more elusive, even for deterministic ODEs [1, 7, 19, 21, 29]. Our aim here is not to contribute to this debate but rather to extend existing pragmatic definitions of stiffness of deterministic ODEs to the random case. To be specific, we provide a few such definitions for deterministic ODEs in section 2.1 and reformulate them for the random setting in section 2.2.

2.1. Stiffness of deterministic ODEs. Consider a deterministic analog of stochastic ODEs (1.1),

$$(2.1) \quad \begin{cases} \frac{d\bar{\mathbf{x}}}{dt}(t) = \bar{\mathbf{f}}(t, \bar{\mathbf{x}}(t)), & t \in (0, T], \\ \bar{\mathbf{x}}(0) = \bar{\mathbf{x}}_0, \end{cases}$$

where $\bar{\mathbf{f}}$ is a vector function nonlinear in $\bar{\mathbf{x}}(t) \in \mathbb{R}^d$ and $\bar{\mathbf{x}}_0 \in \mathbb{R}^d$ is the initial value of $\bar{\mathbf{x}}(t)$. A first-order Taylor expansion around a particular solution, $\bar{\mathbf{x}}_p(t)$, of (2.1) approximates the latter with

$$(2.2) \quad \begin{cases} \frac{d\bar{\mathbf{x}}}{dt} = \frac{d\bar{\mathbf{x}}_p}{dt} + \bar{\mathbf{J}}(t)(\bar{\mathbf{x}} - \bar{\mathbf{x}}_p), & t \in (0, T], \\ \bar{\mathbf{x}}(0) = \bar{\mathbf{x}}_0. \end{cases}$$

Eigenvalues $\bar{\lambda}(t)$ of the Jacobian matrix,

$$(2.3) \quad \bar{\mathbf{J}}(t) \triangleq [\nabla_{\mathbf{y}} \bar{\mathbf{f}}(t, \mathbf{y})]_{\mathbf{y}=\bar{\mathbf{x}}_p},$$

can be used to define the stiffness of ODEs (2.1) as follows [28].

DEFINITION 2.1. *ODEs (2.1) are stiff if the real parts of eigenvalues $\bar{\lambda}(t)$ of the Jacobian $\bar{\mathbf{J}}(t)$ satisfy the condition*

$$(2.4) \quad \max_{\bar{\lambda}} \{\Re(-\bar{\lambda}(t))\} \gg \max_{\bar{\lambda}} \{\Re(\bar{\lambda}(t))\}$$

for every t in (a subinterval of) $[0, T]$.

Since the Jacobian matrix $\bar{\mathbf{J}}(t)$ in (2.3) depends on the particular solution $\bar{\mathbf{x}}_p$, it might not be unique. An alternative definition is given in terms of the (readily computable) stiffness ratio,

$$\bar{s}(t) = \frac{\max_{\bar{\lambda}} \{|\Re(\bar{\lambda}(t))|\}}{\min_{\bar{\lambda}} \{|\Re(\bar{\lambda}(t))|\}}.$$

This workable definition of stiffness reads as follows [21].

DEFINITION 2.2. *ODEs (2.1) are stiff if eigenvalues $\bar{\lambda}(t)$ of the Jacobian $\bar{\mathbf{J}}(t)$ satisfy the conditions*

$$(2.5) \quad \Re(\bar{\lambda}(t)) < 0 \quad \forall \bar{\lambda}(t) \quad \text{and} \quad \bar{s}(t) \gg 1.$$

Yet another way to define the stiffness of ODEs (2.1) is in terms of a Lipschitz constant \bar{L} [21]. Let us assume that the function $\bar{f}(t, \bar{\mathbf{x}}(t))$ in (2.1) satisfies the Lipschitz condition,

$$(2.6) \quad \|\bar{\mathbf{f}}(t, \bar{\mathbf{u}}) - \bar{\mathbf{f}}(t, \bar{\mathbf{v}})\| \leq \bar{L} \|\bar{\mathbf{u}} - \bar{\mathbf{v}}\| \quad \forall \bar{\mathbf{u}}, \bar{\mathbf{v}} \in \mathbb{R}^d,$$

where $\|\cdot\|$ is a vector norm in \mathbb{R}^d . Choose \bar{L} as

$$(2.7) \quad \bar{L} = \|\bar{\mathbf{J}}(t)\| \geq \rho(\bar{\mathbf{J}}(t)) \triangleq \max_{\bar{\lambda}} \{|\bar{\lambda}(t)|\},$$

where $\|\cdot\|$ denotes the induced operator norm when applied to a matrix and $\rho(\cdot)$ is the spectral radius. The phrase “systems with large Lipschitz constants” refers to the following definition of stiffness [21].

DEFINITION 2.3. *ODEs (2.1) are stiff if the Lipschitz constant \bar{L} is large enough.*

2.2. Stiffness of random ODEs. An intuitive, albeit unworkable, definition of stiffness of a random ODE is as follows [28].

DEFINITION 2.4. *Random ODEs (1.1) are stiff with probability $P_0 > 0$ if*

$$\mathbb{P}\{\omega : \text{Deterministic realizations of (1.1) corresponding to } \omega \in \Omega \text{ are stiff}\} = P_0.$$

We use the above to formulate computable analogs of Definitions 2.1–2.4 in terms of the random Jacobian matrix,

$$(2.8) \quad \mathbf{J}(t, \omega) \triangleq [\nabla_{\mathbf{y}} \mathbf{f}(t, \boldsymbol{\xi}(\omega), \mathbf{y})]_{\mathbf{y}=\mathbf{x}_p(t, \omega)}.$$

Similar to (2.1), the latter arises in the course of linearization of (1.1a) around $\mathbf{x}_p(t, \omega)$, a particular solution of (1.1) under an appropriate measure,

$$(2.9) \quad \frac{d\mathbf{x}}{dt}(t, \omega) = \frac{d\mathbf{x}_p}{dt}(t, \omega) + \mathbf{J}(t, \omega)(\mathbf{x} - \mathbf{x}_p), \quad t \in (0, T].$$

As in the deterministic case, the random Jacobian matrix $\mathbf{J}(t)$ in (2.9) depends on the particular solution \mathbf{x}_p and, hence, might not be unique.

DEFINITION 2.5. *Random ODEs (1.1) are stiff with probability $P_0 > 0$ if eigenvalues $\lambda(t, \omega)$ of the Jacobian $\mathbf{J}(t, \omega)$ satisfy*

$$(2.10) \quad \mathbb{P}\{\max_{\lambda} [\Re(-\lambda)] \gg \max_{\lambda} [\Re(\lambda)]\} = P_0$$

for every t in (a subinterval of) $[0, T]$.

DEFINITION 2.6. *Random ODEs (1.1) are stiff with probability $P_0 > 0$ if eigenvalues $\lambda(t, \omega)$ of the Jacobian $\mathbf{J}(t, \omega)$ satisfy*

$$(2.11) \quad \mathbb{P}\{\Re(\lambda(t)) < 0 \quad \forall \lambda \text{ and } s(t, \omega) \gg 1\} = P_0,$$

where the random stiffness ratio $s(t, \omega)$ is defined in analogy with its deterministic counterpart.

DEFINITION 2.7. *Assume that the deterministic vector function \mathbf{f} in random ODEs (1.1) satisfies the Lipschitz condition*

$$(2.12) \quad \|\mathbf{f}(t, \boldsymbol{\xi}(\omega), \mathbf{u}) - \mathbf{f}(t, \boldsymbol{\xi}(\omega), \mathbf{v})\| \leq L(\omega) (\|\mathbf{u} - \mathbf{v}\|), \quad \omega \in \Omega,$$

for all $\mathbf{u}, \mathbf{v} \in \mathbb{R}^d$ in every realization $\omega \in \Omega$. Then random ODEs (1.1) are stiff with probability $P_0 > 0$ if the Lipschitz constant $L(\omega)$ is large with probability $P_0 > 0$.

Remark 2.1. Given the lack of a universally accepted definition of stiffness even in the deterministic setting [7, 19, 21, 22, 29], it is futile, if not outright impossible, to choose the most adequate one among Definitions 2.4–2.7. Some of their known weaknesses are as follows. A limitation of Definition 2.1—and, hence, of Definition 2.5—is that the eigenvalues of the Jacobian matrix $\bar{\mathbf{J}}(t)$ in (2.3)—or of the Jacobian matrix $\mathbf{J}(t, \omega)$ in (2.8)—do not provide a complete description of an exact solution to the original problem [29]. A shortcoming of Definition 2.2—and, hence, of Definition 2.6—is that a system might be stiff yet have the stiffness ratio $\bar{s} = 1$ [22]; conversely, the stiffness ratio \bar{s} can be arbitrarily large (e.g., if the real part of the smallest eigenvalue is close to 0) even when a system is not stiff [21, 29]. A weakness of Definition 2.3—and, hence, of Definition 2.7—stems from the ambiguity of the adjective “large enough” used to characterize the Lipschitz constant \bar{L} in (2.7) or its random counterpart $L(\omega)$ in (2.12) [21].

Remark 2.2. Definitions 2.1–2.7 rely on local linearization of a nonlinear system and involve a local particular solution. The veracity of these definitions is subject to ongoing debate even for linear problems (Remark 2.1) and more so for nonlinear problems.

3. gPC with MIRK for stiff random ODEs. In section 3.1, we formulate a probabilistic model for the parameters $\xi(\omega)$ in (1.1). Sections 3.2 and 3.3 contain a brief overview of the gPC method for solving random ODEs (1.1) and the MIRK scheme for solving the resulting gPC equations, respectively.

3.1. Random parameters. Random variables $\xi(\omega)$ in (1.1) can represent uncertain model parameters and are characterized by a joint probability density function (PDF) $\rho_\xi : \mathbb{R}^N \rightarrow [0, +\infty)$. Alternatively, they can arise from a representation of a temporally varying model parameter $\gamma(t, \omega)$ via, e.g., a truncated Karhunen–Loève expansion [3, 17, 34, 41],

$$(3.1) \quad \gamma(t, \omega) \approx \mathbb{E}\{\gamma\} + \sum_{i=1}^N \sqrt{\mu_i} \phi_i(t) \xi_i(\omega).$$

Here, $\mathbb{E}\{\cdot\}$ denotes the ensemble mean operator defined below, and μ_i and ϕ_i are the eigenvalues and eigenfunctions of a covariance function $C(t, \tau) \triangleq \text{cov}(\gamma(t, \omega), \gamma(\tau, \omega))$, respectively. In this setting, $\xi(\omega) = \{\xi_1, \dots, \xi_N\}$ are mutually uncorrelated identically distributed random variables with

$$(3.2) \quad \mathbb{E}\{\xi_i\} \triangleq \int \Xi_i \rho_\xi(\Xi) d\Xi = 0, \quad \mathbb{E}\{\xi_i \xi_j\} \triangleq \int \Xi_i \Xi_j \rho_\xi(\Xi) d\Xi = \delta_{ij},$$

where δ_{ij} is the Kronecker delta function.

In the former case, wherein random variables $\xi(\omega)$ are correlated model parameters, one can use the Rosenblatt transform (e.g., section 4.1 in [35]) to map $\xi(\omega)$ onto a set of independent, identically distributed random variables $\{\xi'_1, \dots, \xi'_N\}$. Consequently, without loss of generality, we take random variables $\xi(\omega)$ in (1.1) to be mutually uncorrelated and to satisfy (3.2). The PDF $\rho_{\xi_i}(\Xi_i)$ of the i th random variable ξ_i is computed as the marginal of the joint PDF $\rho_\xi(\Xi)$.

3.2. gPC approximation. Let $\psi_{\alpha_i}(\xi_n)$ be a univariate orthogonal polynomial of degree $\alpha_i \in \mathbb{N}^+ \cup \{0\}$ in ξ_n , i.e.,

$$(3.3) \quad \int \psi_{\alpha_i}(\Xi_n) \psi_{\alpha_j}(\Xi_n) \rho_{\xi_n}(\Xi_n) d\Xi_n = \delta_{ij}.$$

Then the N -variate orthogonal polynomials of degree up to p are defined as

$$(3.4) \quad \Psi_\alpha(\xi) = \prod_{i=1}^N \psi_{\alpha_i}(\xi_i), \quad \alpha_1 + \alpha_2 + \dots + \alpha_N \leq p,$$

where $\alpha = (\alpha_1, \alpha_2, \dots, \alpha_N)$ is a multi-index. The isotropic total degree set of order p , $\{\Psi_\alpha(\xi)\}_{\alpha=1}^M$, forms a gPC basis. The number of the gPC basis functions is determined by

$$(3.5) \quad M = \frac{(N + p)!}{N! p!}.$$

The PDF $\rho_{\boldsymbol{\xi}}(\boldsymbol{\Xi})$ determines the type of gPC; a proper choice of polynomials often yields an exponential convergence rate [32, 33, 34, 41].

The coefficients $\mathbf{x}_1(t), \dots, \mathbf{x}_M(t)$ of a gPC approximation,

$$(3.6) \quad \check{\mathbf{x}}(t, \boldsymbol{\xi}) = \sum_{i=1}^M \mathbf{x}_i(t) \Psi_i(\boldsymbol{\xi}),$$

to the solution $\mathbf{x}(t, \omega)$ of random stiff ODEs (1.1) are obtained by replacing $\mathbf{x}(t, \omega)$ with $\check{\mathbf{x}}(t, \boldsymbol{\xi})$ in (1.1) and projecting the result onto the gPC basis.¹ This procedure yields the gPC equations (a system of coupled deterministic ODEs)

$$(3.7) \quad \begin{cases} \frac{d\mathbf{x}_k}{dt} = \mathbb{E} \left\{ \Psi_k(\boldsymbol{\xi}) \mathbf{f} \left(t, \boldsymbol{\xi}, \sum_{i=1}^M \mathbf{x}_i(t) \Psi_i(\boldsymbol{\xi}) \right) \right\}, & t \in (0, T], \\ \mathbf{x}_k(0) = \mathbb{E} \{ \Psi_k(\boldsymbol{\xi}) \varphi(\boldsymbol{\xi}) \} \end{cases}$$

for $k = 1, \dots, M$. Let $\mathbf{y}(t) = (\mathbf{x}_1, \dots, \mathbf{x}_M)^\top$ with $\mathbf{y}(0) = \mathbf{y}_0$ and

$$\mathbf{y}_0 = [\mathbb{E} \{ \Psi_1(\boldsymbol{\xi}) \varphi(\boldsymbol{\xi}) \}, \dots, \mathbb{E} \{ \Psi_M(\boldsymbol{\xi}) \varphi(\boldsymbol{\xi}) \}]^\top.$$

Furthermore, let $\mathbf{z}(t, \mathbf{y}) = (\mathbf{z}_1, \dots, \mathbf{z}_M)^\top$ with

$$\mathbf{z}_k(t, \mathbf{y}) = \mathbb{E} \left\{ \Psi_k(\boldsymbol{\xi}) \mathbf{f} \left(t, \boldsymbol{\xi}, \sum_{i=1}^M x_i(t) \Psi_i(\boldsymbol{\xi}) \right) \right\}.$$

Then a compact form of (3.7) is

$$(3.8) \quad \begin{cases} \frac{d\mathbf{y}}{dt} = \mathbf{z}(t, \mathbf{y}), & t \in (0, T], \\ \mathbf{y}(0) = \mathbf{y}_0. \end{cases}$$

Given the stiffness of (1.1), it is necessary to analyze the stiffness of the gPC equations (3.8). Before carrying out such an analysis, we describe a class of numerical techniques—parallel MIRK schemes—that can efficiently handle the possible stiffness of the gPC equations (3.8).

3.3. Parallel MIRK schemes. The size of the vectors in the gPC equations (3.8) is equal to $d \cdot M$. It increases with both the number of the random variables, N , and the highest order of the gPC basis, p . When N and p reach a certain threshold, the gPC method becomes more expensive than standard Monte Carlo; this performance degradation is referred to as the curse of dimensionality of gPC. Parallel MIRK schemes can be used to alleviate the potentially high cost of solving both the gPC equations (3.8) and Monte Carlo realizations of the random ODE (1.1).

In application to (3.8), a MIRK scheme of stage St takes the form

$$(3.9) \quad \mathbf{y}_{n+1} = \mathbf{y}_n + h \sum_{r=1}^{St} b_r \mathbf{z}(t_n + c_r h, \mathbf{Y}_r), \quad n \geq 0,$$

¹Other possible choices of the total degree multi-index set include an anisotropic total degree set or a hyperbolic cross set.

where \mathbf{y}_n is an approximation of $\mathbf{y}(t)$ at time $t_n = nh$, h is the step size, $c_r = v_r + \sum_{j=1}^{\text{St}} x_{r,j}$, $x_{i,j}$ are elements of an $\text{St} \times \text{St}$ strictly lower triangular matrix, and

$$(3.10) \quad \mathbf{Y}_r = (1 - v_r)\mathbf{y}_n + v_r\mathbf{y}_{n+1} + h \sum_{j=1}^{r-1} x_{r,j}\mathbf{z}(t_n + c_jh, \mathbf{Y}_j).$$

A choice of the constants $\{b_r, c_r, v_r, x_{i,j}\}$ determines a particular MIRK scheme. The implicit scheme (3.9) for \mathbf{y}_{n+1} is solved via the Newton iteration,

$$(3.11a) \quad \mathbf{y}_{n+1}^{(l+1)} = \mathbf{y}_{n+1}^{(l)} + \Delta\mathbf{y}_{n+1}^{(l)}, \quad l = 0, 1, \dots,$$

in which the increment $\Delta\mathbf{y}_{n+1}^{(l)}$ is determined from the relation

$$(3.11b) \quad \mathbf{J}_F(\mathbf{y}_{n+1}^{(l)})\Delta\mathbf{y}_{n+1}^{(l)} = -\mathbf{F}(\mathbf{y}_{n+1}^{(l)}),$$

with

$$(3.11c) \quad \mathbf{F}(\mathbf{y}_{n+1}) \triangleq \mathbf{y}_{n+1} - \mathbf{y}_n - h \sum_{r=1}^{\text{St}} b_r\mathbf{z}(t_n + c_rh, \mathbf{Y}_r)$$

and the Jacobian matrix

$$(3.11d) \quad \mathbf{J}_F(\mathbf{y}_{n+1}^{(l)}) \triangleq [\nabla_{\mathbf{y}}\mathbf{F}(\mathbf{y})]_{\mathbf{y}=\mathbf{y}_{n+1}^{(l)}}.$$

A parallel implementation of the MIRK schemes represents the inverse of $\mathbf{J}_F(\mathbf{y}_{n+1}^{(l)})$ as a partial fraction expansion [38],

$$(3.12a) \quad \mathbf{J}_F^{-1}(\mathbf{y}_{n+1}^{(l)}) = \sum_{i=1}^{\text{St}} C_i(\mathbf{I} - B_i h \mathbf{J}_z(\mathbf{y}_{n+1}^{(l)}))^{-1},$$

where \mathbf{I} is the identity matrix,

$$(3.12b) \quad \mathbf{J}_z(\mathbf{y}_{n+1}^{(l)}) \triangleq [\nabla_{\mathbf{y}}\mathbf{z}(t_{n+1}, \mathbf{y})]_{\mathbf{y}=\mathbf{y}_{n+1}^{(l)}},$$

and

$$(3.12c) \quad C_i = \frac{B_i^{\text{St}-1}}{\prod_{j=1, j \neq i}^{\text{St}} (B_i - B_j)}.$$

A choice of the constants $\{B_i\}$ depends on the stability function of a parallel MIRK scheme. For example, the MIRK332L scheme is characterized by [38]

c_1	v_1	$x_{1,1}$	\cdots	$x_{1,s}$	\Rightarrow	1	1	0	0	0
\vdots	\vdots	\vdots	\vdots	\vdots		$\frac{5}{24}$	$\frac{215}{576}$	$-\frac{95}{576}$	0	0
c_s	v_s	$x_{s,1}$	\cdots	$x_{s,s}$		$\frac{7}{9}$	$\frac{241}{81}$	$-\frac{1414}{1539}$	$-\frac{656}{513}$	0
		b_1	\cdots	b_s				$\frac{1}{76}$	$\frac{384}{779}$	$\frac{81}{164}$

and $B_1 = 1$, $B_2 = 1/4$, $B_3 = 5/12$. This scheme has $\text{St} = 3$ stages, of order 3 (i.e., its local error is $\mathcal{O}(h^4)$) and stage order 2; it is L-stable.

Using (3.12) in the Newton iteration (3.11) gives

$$(3.13) \quad \mathbf{y}_{n+1}^{(l+1)} = \mathbf{y}_{n+1}^{(l)} + \sum_{i=1}^{\text{St}} C_i \Delta_i \mathbf{y}_{n+1}^{(l)}, \quad l = 0, 1, \dots,$$

with the increments $\Delta_i \mathbf{y}_{n+1}^{(l)}$ computed from

$$(3.14) \quad (\mathbf{I} - B_i h \mathbf{J}_z(\mathbf{y}_{n+1}^{(l)})) \Delta_i \mathbf{y}_{n+1}^{(l)} = -\mathbf{F}(\mathbf{y}_{n+1}^{(l)}), \quad i = 1, \dots, \text{St}.$$

The resulting Newton iteration for obtaining \mathbf{y}_{n+1} in (3.9)—the main computational task of a MIRK scheme—can now be done in parallel on St processors.

Given the potential stiffness of the gPC equations (3.8), we will use the parallel MIRK family that has a desirable stability, e.g., A-stability or L-stability, to solve (3.8). The choice of a stability type is problem dependent. Efficiency, stability, and order accuracy of various parallel MIRK schemes are discussed in [6, 25, 38].

Remark 3.1. MIRK schemes, introduced in [8, 25], strive to achieve a balance between the high accuracy and efficiency of IRKs. Order results for and a brief overview of MIRK schemes can be found in [6]. A subclass of parallelizable MIRK schemes was investigated in [36]; having stage order 1, these methods are susceptible to order reduction [6, 28] (see also the results of our numerical experiments in sections 5.1 and 5.2). Subsequent improvements of parallel MIRK methods [38] resulted in schemes with stage order 2 or 3 (see [37] for a survey of parallel MIRK schemes). We investigate the parallel MIRK schemes [38] because they can ultimately be used in high-performance computing.

4. Analysis of stiffness. A theoretical analysis of the stiffness of random ODEs is presented in section 4.1. In section 4.2, we establish a relationship between the Jacobian of random ODEs and the corresponding gPC equations. In section 4.3, this relationship is used to predict the stiffness of the gPC equations, allowing one to design an appropriate numerical scheme for the latter.

4.1. Stiffness analysis of random ODEs. Following Definition 2.7, we consider random ODEs (1.1) whose Lipschitz constant $L(\omega) \triangleq \|\mathbf{J}(t, \omega)\|$ is sufficiently large with probability P_0 .

Remark 4.1. Some authors find the phrase “systems with large Lipschitz constants” and, hence, Definitions 2.3 and 2.7 to be not entirely satisfactory [1, 7, 19, 21, 29]. Considering that all existing definitions of stiffness are somewhat arbitrary [1, 7, 19, 21, 29], we will use Definition 2.7 as a working albeit imperfect definition of stiffness.

Let J_{ij} with $i, j = 1, \dots, d$ denote components of the random Jacobian matrix $\mathbf{J}(t, \omega)$ in (2.8). For the sake of simplicity, we consider the matrix norm induced by the ℓ_1 norm.² A useful property of the Jacobian $\mathbf{J}(t, \omega)$ is given by the following lemma.

LEMMA 4.1. *Let the $d \times d$ Jacobian matrix $\mathbf{J}(t, \omega)$ be such that*

$$(4.1) \quad \mathbb{P}\{\Omega_1\} > 0, \quad \Omega_1 \triangleq \{\omega : \|\mathbf{J}(t, \omega)\|_1 \geq L_1\},$$

²The reliance on the ℓ_1 norm facilitates the straightforward calculation of the norms of the relevant Jacobian matrices. Our analysis and conclusions are readily portable to the ℓ_∞ norm; extensions to other norms, e.g., the ℓ_2 norm, are more challenging.

where L_1 is a positive constant. Then, for any $\omega \in \Omega_1$, there exists an element $J_{i_0j_0}(t, \omega)$ of $\mathbf{J}(t, \omega)$ for which

$$(4.2) \quad |J_{i_0j_0}| \geq L_1/d;$$

the values of i_0 and j_0 depend on ω .

Proof. For any $\omega \in \Omega_1$,

$$(4.3) \quad \|\mathbf{J}(t, \omega)\|_1 = \max_{1 \leq j \leq d} \sum_{i=1}^d |J_{ij}| \geq L_1.$$

Hence, there exists a column $j_0 : 1 \leq j_0 \leq d$ such that

$$(4.4) \quad \sum_{i=1}^d |J_{ij_0}| \geq L_1,$$

where j_0 depends on ω . It therefore follows that there exists an index $i_0 : 1 \leq i_0 \leq d$ for which

$$(4.5) \quad |J_{i_0j_0}| \geq L_1/d,$$

where i_0 depends on ω . This completes the proof. □

Lemma 4.1 implies that if random ODEs (1.1) were stiff with nonzero probability in the sense of Definition 2.7, then the event “the Jacobian matrix \mathbf{J} has an element whose absolute value is sufficiently large” occurs with nonzero probability. If one picks the constant L_1 in (4.1) to be sufficiently large for L_1/d to be sufficiently large as well, then $J_{i_0j_0}$ is the element of the Jacobian of (1.1), whose absolute value is large enough. This occurs for any $\omega : \|\mathbf{J}(t, \omega)\|_1 \geq L_1$, i.e., with probability no less than $\mathbb{P}\{\omega : \|\mathbf{J}(t, \omega)\|_1 \geq L_1\}$. The following theorem provides a probabilistic lower bound on the Jacobian $\|\mathbf{J}(t, \omega)\|_1$.

THEOREM 4.1. *Assume that the Jacobian $\mathbf{J}(t, \omega)$ has an element $J_{i_0j_0}$ for which*

$$(4.6) \quad \mathbb{P}\{\Omega_2\} > 0, \quad \Omega_2 \triangleq \{\omega : |J_{i_0j_0}| \geq L_2\},$$

where L_2 is a positive number. Then

$$(4.7) \quad \mathbb{P}\{\omega : \|\mathbf{J}(t, \omega)\|_1 \geq L_2\} \geq \mathbb{P}\{\Omega_2\}.$$

Proof. It follows from (4.6) that, for all $\omega \in \Omega_2$,

$$(4.8) \quad |J_{i_0j_0}| \geq L_2.$$

According to the definition of the matrix norm induced by the ℓ_1 norm,

$$(4.9) \quad \|\mathbf{J}(t, \omega)\|_1 = \max_{1 \leq j \leq d} \sum_{i=1}^d |J_{ij}|.$$

Hence, for every time t , the inequality

$$(4.10) \quad \|\mathbf{J}(t, \omega)\|_1 = \max_{1 \leq j \leq d} \sum_{i=1}^d |J_{ij}| \geq \sum_{i=1}^d |J_{ij}|$$

holds for any index $j : 1 \leq j \leq d$. It follows from (4.10) that, for every time t , the inequalities

$$(4.11) \quad \|\mathbf{J}(t, \omega)\|_1 = \max_{1 \leq j \leq d} \sum_{i=1}^d |J_{ij}| \geq \sum_{i=1}^d |J_{ij}| \geq |J_{ij}|$$

hold for any index $i : 1 \leq i \leq d$. Accounting for (4.8),

$$(4.12) \quad \|\mathbf{J}(t, \omega)\|_1 = \max_{1 \leq j \leq d} \sum_{i=1}^d |J_{ij}| \geq \sum_{i=1}^d |J_{ij_0}| \geq |J_{i_0 j_0}| \geq L_2 \quad \forall \omega \in \Omega_2.$$

This yields

$$(4.13) \quad \mathbb{P}\{\omega : \|\mathbf{J}(t, \omega)\|_1 \geq L_2\} \geq \mathbb{P}\{\Omega_2\},$$

which completes the proof. □

Remark 4.2. Theorem 4.1 implies that if one finds an element of the Jacobian \mathbf{J} whose absolute value is sufficiently large with probability $P_1 > 0$, then random ODEs (1.1) are stiff with probability no less than P_1 in the sense of Definition 2.7. This result provides a simple and direct way to determine whether random ODEs are stiff. Theorem 4.1 also states that if the Jacobian norm $\|\mathbf{J}(t, \omega)\|_1$ is sufficiently large with probability no less than P_1 , then it can serve as the Lipschitz constant in (2.12), thus ensuring that random ODEs (1.1) are stiff with probability no less than P_1 .

Remark 4.3. A priori determination of the stiffness of random ODEs like (1.1) is important for the selection of an appropriate numerical method. While much of our analysis centers on gPC, this observation is equally valid for other approaches such as Monte Carlo methods and stochastic collocation on sparse grids. If (1.1) were stiff, these and other sampling methods of stochastic computation call for the use of a proper stiff solver in each deterministic realization of (1.1). Doing otherwise would lead to erroneous results, e.g., highly unstable solutions obtained from an A-stable method [6, 14, 15, 19, 28].

4.2. Relation between Jacobians of random ODEs and gPC equations.

A first-order Taylor series expansion of (3.8) is

$$(4.14) \quad \begin{cases} \frac{d\mathbf{y}}{dt} = \frac{d\mathbf{y}_p}{dt} + \tilde{\mathbf{J}}(t)(\mathbf{y} - \mathbf{y}_p), & t \in (0, T], \\ \mathbf{y}(0, \omega) = \mathbf{y}_0(\omega), \end{cases}$$

where $\mathbf{y}_p(t, \omega)$ is a particular solution of (3.8) and $\tilde{\mathbf{J}}(t) \triangleq [\nabla_{\mathbf{y}} \mathbf{z}(t, \mathbf{y})]_{\mathbf{y}=\mathbf{y}_p} \in \mathbb{R}^{(Md) \times (Md)}$ is the Jacobian matrix written as

$$(4.15a) \quad \tilde{\mathbf{J}}(t) \triangleq \begin{pmatrix} \tilde{\mathbf{J}}_{11} & \tilde{\mathbf{J}}_{12} & \cdots & \tilde{\mathbf{J}}_{1M} \\ \tilde{\mathbf{J}}_{21} & \tilde{\mathbf{J}}_{22} & \cdots & \tilde{\mathbf{J}}_{2M} \\ \vdots & \vdots & \ddots & \vdots \\ \tilde{\mathbf{J}}_{M1} & \tilde{\mathbf{J}}_{M2} & \cdots & \tilde{\mathbf{J}}_{MM} \end{pmatrix}, \quad \tilde{\mathbf{J}}_{ij}(t, \omega) \in \mathbb{R}^{d \times d}.$$

Accounting for (3.7) and (3.8), the matrices $\tilde{\mathbf{J}}_{ij}$ are given by

$$(4.15b) \quad \tilde{\mathbf{J}}_{ij} = \mathbb{E}\{\Psi_i(\boldsymbol{\xi}) \mathbf{J}(t, \omega) \Psi_j(\boldsymbol{\xi})\}, \quad 1 \leq i, j \leq M.$$

Relation (4.15) links the Jacobian of random ODE (1.1), $\mathbf{J}(t, \omega)$ first introduced in (2.8), and the Jacobian of the corresponding gPC equations (3.8), $\tilde{\mathbf{J}}(t)$. Properties of the matrix norm induced by the ℓ_1 norm give rise to the following lemma.

LEMMA 4.2. *The Jacobians of random ODEs (1.1) and the corresponding gPC equations (3.8), $\mathbf{J}(t, \omega)$ and $\tilde{\mathbf{J}}(t)$, respectively, satisfy the condition*

$$(4.16) \quad \|\tilde{\mathbf{J}}(t)\|_1 \geq |\mathbb{E}\{J_{ij}(t, \omega)\}| \quad \forall i, j : 1 \leq i, j \leq d.$$

Proof. The properties of the matrix norm induced by the ℓ_1 norm yield

$$(4.17) \quad \begin{aligned} \|\tilde{\mathbf{J}}\|_1 &= \max_{1 \leq n \leq Md} \sum_{m=1}^{Md} |\kappa_{mn}| \geq \max_{(l-1)d+1 \leq n \leq ld} \sum_{m=(k-1)d+1}^{kd} |\kappa_{mn}| \\ &= \|\tilde{\mathbf{J}}_{kl}\|_1 \quad \forall k, l : 1 \leq k, l \leq M, \end{aligned}$$

where κ_{mn} is the element in the m th row and n th column of $\tilde{\mathbf{J}}(t)$. Choosing $k = 1$ and $l = 1$ in (4.17),

$$(4.18) \quad \|\tilde{\mathbf{J}}(t)\|_1 \geq \|\tilde{\mathbf{J}}_{11}\|_1.$$

Since the gPC basis functions $\{\Psi_k(\boldsymbol{\xi})\}$ are orthonormal, $\mathbb{E}\{\Psi_1^2(\boldsymbol{\xi})\} = 1$ or $\Psi_1(\boldsymbol{\xi}) = 1$. Hence, it follows from (4.15b) that

$$(4.19) \quad \tilde{\mathbf{J}}_{11} = \mathbb{E}\{\mathbf{J}(t, \omega)\}.$$

According to (4.11),

$$(4.20) \quad \|\tilde{\mathbf{J}}_{11}\|_1 = \|\mathbb{E}\{\mathbf{J}(t, \omega)\}\|_1 = \max_{1 \leq j \leq d} \sum_{i=1}^d |\mathbb{E}\{J_{ij}\}| \geq \sum_{i=1}^d |\mathbb{E}\{J_{ij}\}| \geq |\mathbb{E}\{J_{ij}\}|$$

for all $i, j : 1 \leq i, j \leq d$. Combining (4.18) with (4.20) yields (4.16), which completes the proof. □

4.3. Stiffness analysis of gPC equations. Definition 2.3 and Lemma 4.2 lead to the following theorem.

THEOREM 4.2. *If the absolute expected value of a certain element, $|\mathbb{E}\{J_{ij}\}|$, of the Jacobian matrix $\mathbf{J}(t, \omega)$ of random ODEs (1.1) is sufficiently large, then the corresponding gPC equations (3.8) are stiff.*

Proof. According to Lemma 4.2, a sufficiently large $|\mathbb{E}\{J_{ij}\}|$ translates into a sufficiently large $\|\tilde{\mathbf{J}}(t)\|_1$. Choosing $\|\tilde{\mathbf{J}}(t)\|_1$ to be the Lipschitz constant of gPC equations (3.8), we conclude that the gPC equations (3.8) are stiff in the sense of Definition 2.3. □

Remark 4.4. Theorem 4.2 provides a direct means to determine whether the gPC equations (3.8) are stiff.

Remark 4.5. If the gPC equations (3.8) are identified to be stiff, appropriate numerical schemes must be used to solve them (see Remark 4.3).

The following corollary is a special case of Theorem 4.1 or Remark 4.2.

COROLLARY 4.1. *Assume that a certain element J_{ij} of the Jacobian matrix $\mathbf{J}(t, \omega)$ of random ODEs (1.1) is such that*

$$(4.21) \quad \mathbb{P}\{\omega : J_{ij} \leq -L_3\} = 1,$$

where L_3 is a sufficiently large positive number. Then random ODEs (1.1) are stiff with probability 1, and the resulting gPC equations are stiff.

Proof. Theorem 4.1 or Remark 4.2 states that random ODEs (1.1) are stiff with probability 1. It follows from (4.21) that

$$(4.22) \quad |\mathbb{E}\{J_{ij}\}| = \left| \int_{\{\omega: J_{ij} \leq -L_3\}} J_{ij} d\mathbb{P}(\omega) \right| \geq L_3.$$

According to Theorem 4.2, the resulting gPC equations are stiff. This completes the proof. \square

5. Numerical experiments. We consider several linear and nonlinear examples to illustrate both the stiffness of random ODEs and the effectiveness of the gPC with parallel MIRK methods. Unless specified otherwise, we use the parallel MIRK332L scheme [38] with step size $h = 0.0001$. When an exact analytical solution $\mathbf{x}(t, \omega)$ is available, its mean and variance are computed via the Gauss quadrature with 15 Gauss points, e.g., [29]. A gPC approximation of the exact solution $\mathbf{x}(t, \omega)$ is

$$(5.1) \quad \hat{\mathbf{x}}(t_k, \boldsymbol{\xi}) = \sum_{k=1}^M \mathbf{y}_k \Psi_k(\boldsymbol{\xi}),$$

where $\{\mathbf{y}_k\}$ are obtained from (3.9). Error measures for the mean and variance of the gPC solution are, respectively, defined as

$$(5.2) \quad \epsilon_m \triangleq \max_{t_k} \|\mathbb{E}\{\mathbf{x}(t_k, \omega)\} - \mathbb{E}\{\hat{\mathbf{x}}(t_k, \boldsymbol{\xi})\}\|_1$$

and

$$(5.3) \quad \epsilon_v \triangleq \max_{t_k} \|\mathbb{E}\{(\mathbf{x}(t_k, \omega) - \mathbb{E}\{\mathbf{x}(t_k, \omega)\})^2\} - \mathbb{E}\{(\hat{\mathbf{x}}(t_k, \boldsymbol{\xi}) - \mathbb{E}\{\hat{\mathbf{x}}(t_k, \boldsymbol{\xi})\})^2\}\|_1.$$

In lieu of the stiffness ratio $\bar{s}(t)$ for the gPC equations, first defined in Definition 2.2, we use a modified stiffness ratio,

$$(5.4) \quad \tilde{s}(t) \triangleq \frac{\max_{\lambda} \{|\Re(\lambda(t))|\}}{\min_{\lambda} \{|\Re(\lambda(t))|\}}$$

regardless of whether $\Re(\lambda(t))$ is negative or not. Here, $\{\lambda(t)\}$ are eigenvalues of the Jacobian matrix, $\tilde{\mathbf{J}}(t)$ in (4.15), of gPC equations (3.8).

5.1. System of linear ODEs. We consider a random counterpart of the Prothero–Robinson problem that is often used to study the order-reduction phenomenon of Runge–Kutta (RK) methods for stiff differential equations [28, 38]. A vector $\mathbf{x}(t, \omega) \in \mathbb{R}^6$ satisfies a system of random ODEs subject to a random initial condition,

$$(5.5a) \quad \begin{cases} \frac{d\mathbf{x}}{dt} = \frac{d\mathbf{x}_p}{dt} + \mathbf{A} \cdot (\mathbf{x} - \mathbf{x}_p), & t \in (0, 1], \\ \mathbf{x}(0, \omega) = \mathbf{x}_p(0, \omega). \end{cases}$$

Here,

$$(5.5b) \quad \mathbf{A} = \text{diag}\{-10^0, -10^1, -10^2, -10^3, -10^4, -10^5\}$$

and

$$(5.5c) \quad \mathbf{x}_p(t, \omega) = \mathbf{1} + 0.2[\sin(t + 0.05\xi_1), \sin(2t + 0.05\xi_2) \dots, \sin(6t + 0.05\xi_6)]^\top,$$

where $\mathbf{1}$ is the six-dimensional vector of 1s and $\boldsymbol{\xi} = \{\xi_1, \dots, \xi_6\}$ are independent random variables with either uniform distribution on $[-1, 1]$ or standard normal distribution. The exact solution of (5.5) is $\mathbf{x}(t, \omega) = \mathbf{x}_p(t, \omega)$.

The Jacobian of (5.5) is $\mathbf{J} = \mathbf{A}$. The element J_{66} of the matrix \mathbf{J} in (5.5b) is such that

$$(5.6) \quad \mathbb{P}\{\omega : J_{66} \leq -10^5\} = 1.$$

Hence, according to Theorem 4.1, Remark 4.2, or Corollary 4.1, random ODEs (5.5) are stiff with probability 1. In solving these equations with gPC, we use Legendre polynomials for uniformly distributed $\boldsymbol{\xi}$ and Hermite polynomials for standard Gaussian $\boldsymbol{\xi}$. Theorem 4.2 or Corollary 4.1 identifies the corresponding gPC equations (3.8) as stiff.

For the random variables $\boldsymbol{\xi}$ distributed uniformly on $[-1, 1]$, gPC equations (3.8) have the modified stiffness ratio $\tilde{s}(t) = 10^5$ and the Lipschitz constant $\|\tilde{\mathbf{J}}(t)\|_1 = 10^5$ for the Legendre chaos of highest order $P = 0, 1, 2,$ or 3 . Such large numbers imply that the gPC equations are stiff, as predicted by Corollary 4.1.

The errors in the mean (ϵ_m) and variance (ϵ_v) of the gPC solution, $\hat{\mathbf{x}}(t, \boldsymbol{\xi})$, are shown in Figure 5.1 as function of the polynomial order P . The error for the mean is $\epsilon_m \sim \mathcal{O}(10^{-12})$. Its insensitivity to the considered values of P is due to the limit of the accuracy of the employed numerical scheme; Table 5.1 elaborates this point further by demonstrating that ϵ_m decreases further as the step size h is reduced. The error for the solution variance, ϵ_v , decreases quickly as P increases, showing the effectiveness of the gPC with parallel MIRK methods.

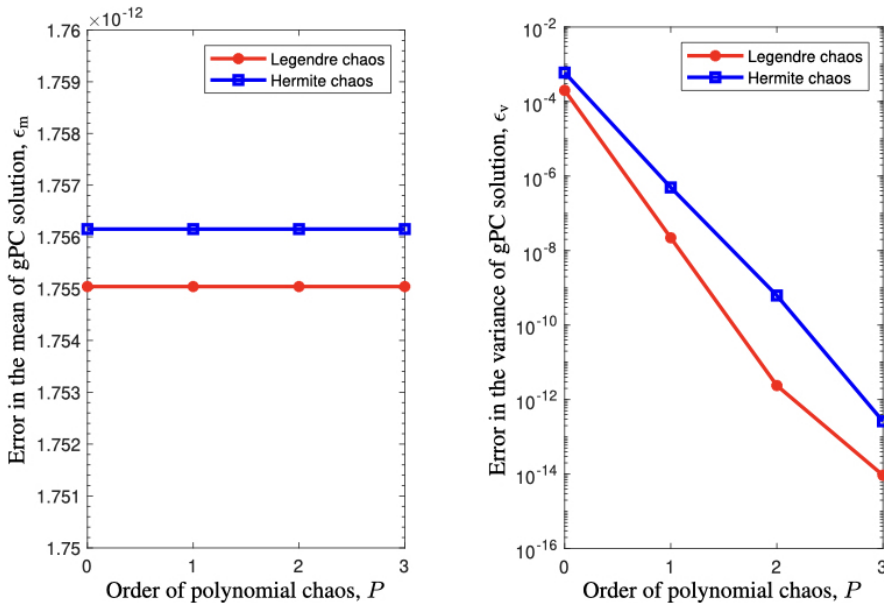


FIG. 5.1. Errors in the mean, ϵ_m , and variance, ϵ_v , of the gPC solution to (5.5) obtained via either Legendre or Hermite chaos of order P with the parallel MIRK332L scheme. The choice of the polynomial type is dictated by the PDF of model inputs $\boldsymbol{\xi}$.

TABLE 5.1

Error, ϵ_m , in computing the mean solution $\mathbb{E}\{\mathbf{x}(t, \omega)\}$ with Legendre and Hermite chaos of order P as function of step size h . The results are identical for $P = 0, \dots, 3$.

	$h = 0.1$	$h = 0.01$	$h = 0.001$	$h = 0.0001$
Legendre	9.533×10^{-5}	3.038×10^{-7}	8.176×10^{-10}	1.755×10^{-12}
Hermite	9.526×10^{-5}	3.036×10^{-7}	8.169×10^{-10}	1.756×10^{-12}

TABLE 5.2

Errors in the mean, ϵ_m , and variance, ϵ_v , of the gPC solution to (5.5) obtained via either Legendre or Hermite chaos of order $P = 3$ with the classical explicit RK method of order 4 as function of step size h . The symbol NaN indicates that the corresponding numerical result is erroneous.

Polynomial	Error	$h = 10^{-1}$	$h = 10^{-2}$	$h = 10^{-3}$	$h = 10^{-4}$	$h = 10^{-5}$
Legendre	ϵ_m	NaN	NaN	NaN	NaN	1.21×10^{-11}
Legendre	ϵ_v	NaN	NaN	NaN	NaN	1.29×10^{-14}
Hermite	ϵ_m	NaN	NaN	NaN	NaN	1.21×10^{-11}
Hermite	ϵ_v	NaN	NaN	NaN	NaN	2.65×10^{-13}

For the standard Gaussian input $\boldsymbol{\xi}$, we found the modified stiffness ratio $\tilde{s}(t) = 10^5$ and the Lipschitz constant $\|\tilde{J}(t)\|_1 = 10^5$ regardless of the Hermite polynomial order $P = 0, \dots, 3$. Hence, the gPC equations are indeed stiff, as predicted a priori by the theory. The errors in the mean and variance of the gPC solution are displayed in Figure 5.1. Similar to the previous example, the error of the mean, ϵ_m , does not decrease with P due to the limit of the accuracy of the numerical scheme employed. That is verified by Table 5.1, which demonstrates the decay of ϵ_m with step size h . Likewise, the error for the variance, ϵ_v , decreases nearly exponentially with P , demonstrating the efficiency of gPC with parallel MIRK methods.

To highlight the numerical challenges of random stiff problems, we compare our MIRK332L solution to (5.5) with that obtained via the classical RK method with the Butcher tableau [18],

$$\begin{array}{c|cccc}
 0 & 0 & 0 & 0 & 0 \\
 \frac{1}{2} & \frac{1}{2} & 0 & 0 & 0 \\
 \frac{1}{2} & 0 & \frac{1}{2} & 0 & 0 \\
 1 & 0 & 0 & 1 & 0 \\
 \hline
 & \frac{1}{6} & \frac{1}{3} & \frac{1}{3} & \frac{1}{6}
 \end{array} ;$$

this explicit RK method is of order 4; i.e., its local error is $\mathcal{O}(h^5)$. In all cases, depending on the PDF of model input $\boldsymbol{\xi}$, we rely on either Legendre or Hermite chaos of the highest order $P = 3$. Table 5.2 shows that the third-order Legendre or Hermite chaos with the fourth-order explicit RK method yields erroneous results, unless the step size h is exceedingly small.

As another possible alternative, we replace the MIRK332L scheme with the Lobatto IIIB method of order 6 [19]. This IRK method has the local error of $\mathcal{O}(h^7)$; it is A-stable but not B-convergent. We study ϵ_m and ϵ_v as functions of step size h , i.e., $\epsilon_m = \epsilon_m(h)$ and $\epsilon_v = \epsilon_v(h)$, and define empirical convergence orders of the Legendre or Hermite chaos as

$$(5.7) \quad p_m \triangleq \frac{1}{\ln 2} \ln \left\{ \left| \frac{\epsilon_m(h)}{\epsilon_m(h/2)} \right| \right\} \quad \text{and} \quad p_v \triangleq \frac{1}{\ln 2} \ln \left\{ \left| \frac{\epsilon_v(h)}{\epsilon_v(h/2)} \right| \right\}.$$

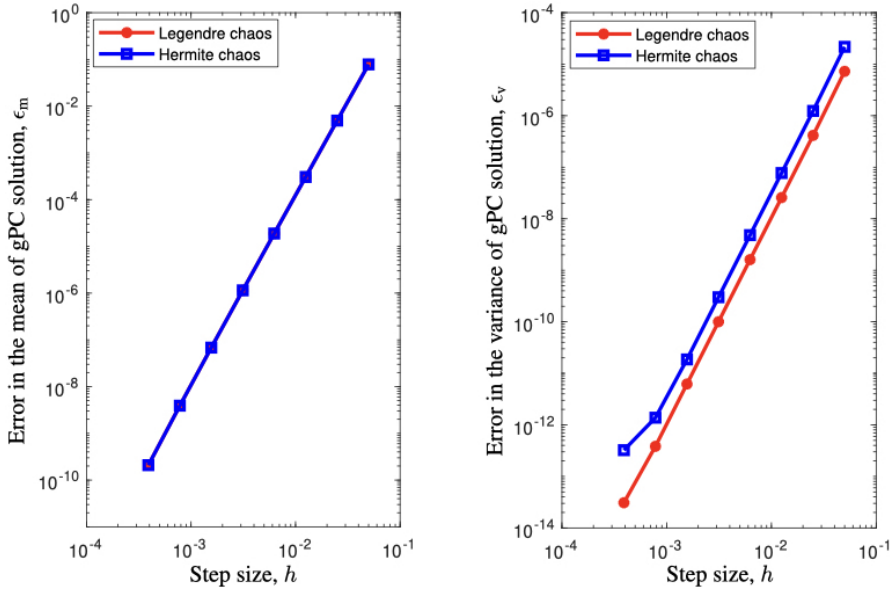


FIG. 5.2. Errors in the mean, ϵ_m , and variance, ϵ_v , of the gPC solution to (5.5) obtained via either Legendre or Hermite chaos of order $P = 3$ with the Lobatto IIIB method of order 6. These errors are plotted as function of step size h .

TABLE 5.3

Empirical convergence orders, p_m , and p_v , of the solution to (5.5) obtained via either Legendre or Hermite chaos of order $P = 3$ with the sixth-order Lobatto IIIB method as function of step size h .

Step size h	$\frac{1}{20}$	$\frac{1}{40}$	$\frac{1}{80}$	$\frac{1}{160}$	$\frac{1}{320}$	$\frac{1}{640}$	$\frac{1}{1280}$	$\frac{1}{2560}$
Legendre p_m		3.992	4.008	4.020	4.038	4.070	4.127	4.227
Legendre p_v		4.129	4.008	4.000	4.005	4.013	4.018	3.634
Hermite p_m		3.992	4.008	4.020	4.038	4.070	4.127	4.227
Hermite p_v		4.130	4.005	4.002	4.004	4.009	3.755	2.093

The errors $\epsilon_m = \epsilon_m(h)$ and $\epsilon_v = \epsilon_v(h)$ are shown in Figure 5.2 and the convergence orders p_m and p_v in Table 5.3. These empirical results show the method’s accuracy of order about 4, a remarkable order reduction of the theoretical order 6. The numerical challenges explored here are closely related to the problem’s stiffness and, hence, demonstrate the need for a proper stiff solver, as commented in Remark 4.3.

5.2. System of nonlinear ODEs. In a nonlinear extension of the randomized Prothero–Robinson problem, $\mathbf{x}(t, \omega) \in \mathbb{R}^6$ is a solution of

$$(5.8) \quad \begin{cases} \frac{d\mathbf{x}}{dt} = \frac{d\mathbf{x}_p}{dt} + \mathbf{A} \cdot \mathbf{f}(\mathbf{x}), & t \in (0, 1], \\ \mathbf{x}(0, \omega) = \mathbf{x}_p(0, \omega), \end{cases}$$

where the vector $\mathbf{x}_p(t, \omega) \in \mathbb{R}^6$ and the matrix $\mathbf{A} \in \mathbb{R}^{6 \times 6}$ are defined in (5.5) and

$$(5.9) \quad \mathbf{f} = (f_1, \dots, f_6)^\top \quad \text{with} \quad f_i = x_i^2 - x_{p_i}^2, \quad i = 1, \dots, 6.$$

The random variables $\boldsymbol{\xi} = (\xi_1, \dots, \xi_6)^\top$ that parameterize \mathbf{x}_p in (5.5c) are mutually independent and have either uniform distribution on $[-1, 1]$ or standard Gaussian distribution. The exact solution of (5.8) is $\mathbf{x}(t, \omega) = \mathbf{x}_p(t, \omega)$.

The Jacobian matrix $\mathbf{J}(t, \omega)$ for (5.8) has zero off-diagonal components, $J_{kn} = 0$ for $k \neq n$, and the diagonal components

$$J_{kk} = -2 \cdot 10^{k-1} \cdot [1 + 0.2 \sin(kt + 0.05\xi_k)], \quad k = 1, \dots, 6.$$

Since $-1 \leq \sin(kt + 0.05\xi_k) \leq 1$ holds with probability 1,

$$(5.10) \quad \mathbb{P}[J_{66} \leq -1.6 \times 10^5] = 1.$$

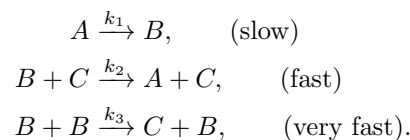
According to Theorem 4.1 (or Remark 4.2 or Corollary 4.1), ODEs (5.8) are stiff with probability 1. According to Theorem 4.2 (or Corollary 4.1), the corresponding gPC equations are stiff.

Figure 5.3 confirms this theoretical observation by exhibiting the modified stiffness ratio $\tilde{s}(t)$ and the Lipschitz constant $\|\tilde{\mathbf{J}}(t)\|_1$ of the gPC equations. Both quantities are time dependent but sufficiently large at all times regardless of the PDF type of $\boldsymbol{\xi}$ and the polynomial order P . The impact of P on both characteristics is slightly more pronounced for the Hermite chaos than for the Legendre one.

Errors in the mean, ϵ_m , and variance ϵ_v , of the gPC solution to (5.8) are displayed in Figure 5.4 for uniform and Gaussian $\boldsymbol{\xi}$. Both error measures decrease quickly with the (Legendre or Hermite) polynomial order P . This demonstrates the effectiveness of gPC with parallel MIRK methods in solving random nonlinear ODEs.

We contrast this performance with the failure of the corresponding solutions obtained by replacing the parallel MIRK method with either the fourth-order explicit RK method (Table 5.4) or the sixth-order Lobatto IIIB method (Figure 5.5 and Table 5.5). The RK method requires a very small step size, $h = 10^{-5}$, to obtain a meaningful solution. As in the linear case considered previously, the order of the Lobatto IIIB method is reduced from 6 to 4 (as indicated by the empirical convergence orders p_m and p_v in Table 5.5). These shortcomings of standard high-order methods demonstrate the need for a proper stiff solver for random problems, as commented in Remark 4.3.

5.3. ODEs of chemical kinetics. Next, we consider a random counterpart of the Robertson problem [7, 19, 30] that is popular in the study of numerical methods for stiff problems in chemical kinetics. The problem deals with slow, fast, and very fast irreversible chemical reactions between species A , B , and C ,



The speed of these reactions is controlled by the rate constants, which we set to $k_1 = 0.04$, $k_2 = 10^4$, and $k_3 = 3 \times 10^7$, all defined in some consistent units. The

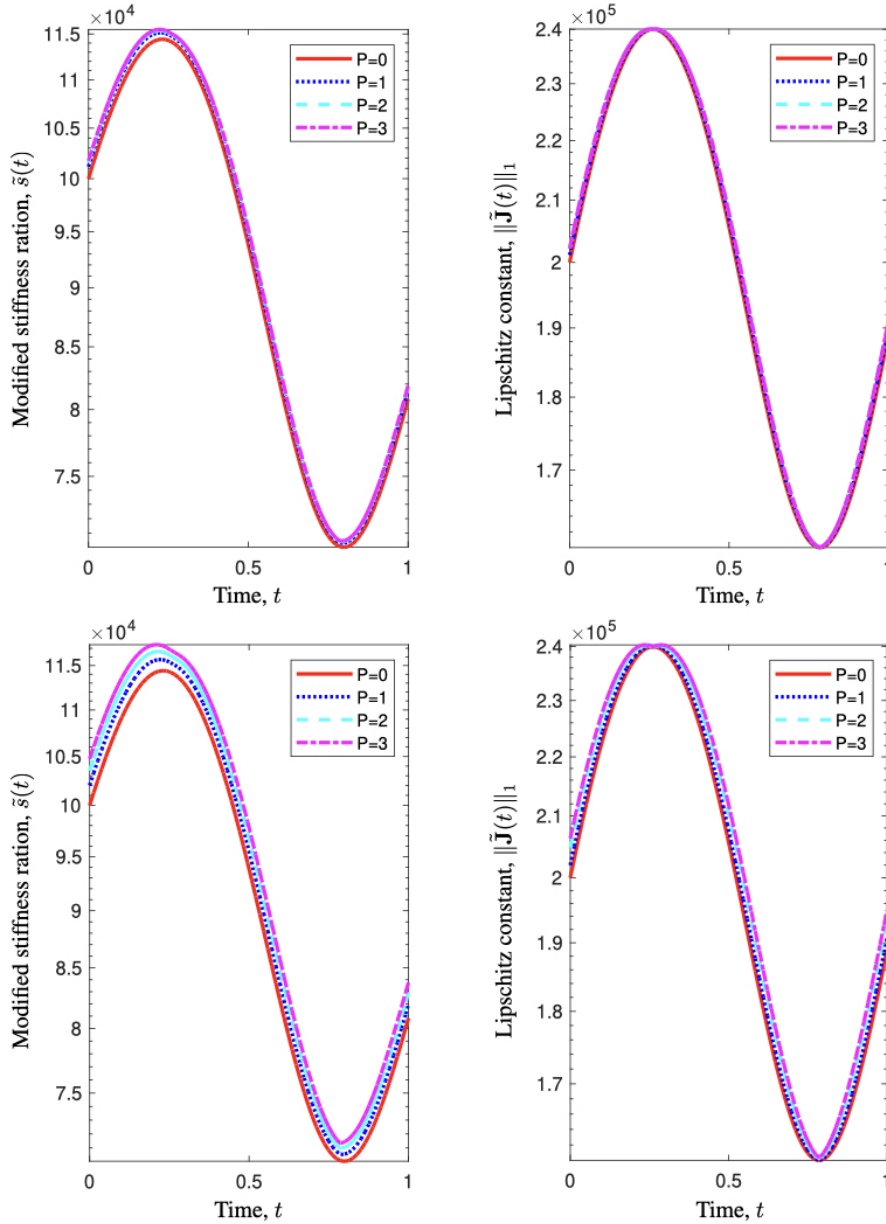


FIG. 5.3. Modified stiffness ratio $\bar{s}(t)$ and the Lipschitz constant $\|\tilde{\mathbf{J}}(t)\|_1$ of the gPC equations for the Legendre (top row) or Hermite (bottom row) chaos of polynomial order P .

concentrations of species A , B , and C , denoted, respectively, by $x_1(t, \omega)$, $x_2(t, \omega)$ and $x_3(t, \omega)$, evolve according to a system of nonlinear ODEs

$$(5.11a) \quad \begin{cases} \frac{dx_1}{dt} = -k_1 x_1 + k_2 x_2 x_3, \\ \frac{dx_2}{dt} = k_1 x_1 - k_2 x_2 x_3 - k_3 x_2^2, \\ \frac{dx_3}{dt} = k_3 x_2^2 \end{cases}$$

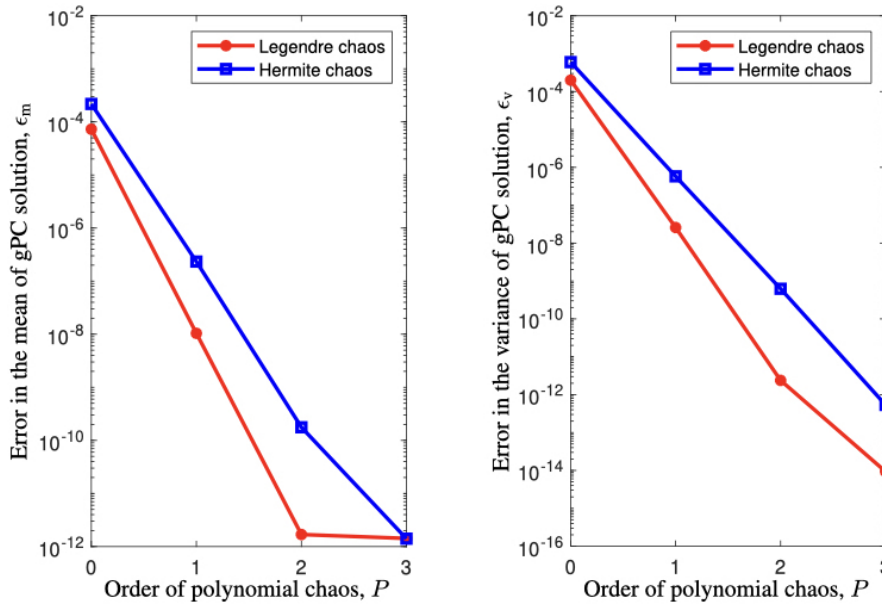


FIG. 5.4. Errors in the mean, ϵ_m , and variance, ϵ_v , of the gPC solution to (5.8) obtained via either Legendre or Hermite chaos of order P with the parallel MIRK332L scheme. The choice of the polynomial type is dictated by the PDF of model inputs ξ .

TABLE 5.4

Errors in the mean, ϵ_m , and variance, ϵ_v , of the gPC solution to (5.8) obtained via either Legendre or Hermite chaos of order $P = 3$ with the classical fourth-order RK method. These errors are presented for several values of step size h . The symbol NaN indicates that the corresponding numerical result is erroneous.

		$h = 10^{-1}$	$h = 10^{-2}$	$h = 10^{-3}$	$h = 10^{-4}$	$h = 10^{-5}$
Legendre	ϵ_m	NaN	NaN	NaN	NaN	2.35×10^{-10}
Legendre	ϵ_v	NaN	NaN	NaN	NaN	6.04×10^{-14}
Hermite	ϵ_m	NaN	NaN	NaN	NaN	2.35×10^{-10}
Hermite	ϵ_v	NaN	NaN	NaN	NaN	5.17×10^{-13}

during the time interval $t \in [0, 1]$. These equations are subject to initial conditions

$$\begin{aligned}
 (5.11b) \quad & \begin{cases} x_1(0, \omega) = 1 - 10^{-6}(1 + 0.05\xi_1) - 0.2(1 + 0.05\xi_2), \\ x_2(0, \omega) = 10^{-6}(1 + 0.05\xi_1), \\ x_3(0, \omega) = 0.2(1 + 0.05\xi_2), \end{cases}
 \end{aligned}$$

where $\xi_1(\omega)$ and $\xi_2(\omega)$ are independent random variables with either uniform distribution on $[-1, 1]$ or standard normal distribution. The reference solution to this problem is obtained via the gPC of order $P = 4$.

The Jacobian matrix $\mathbf{J}(t, \omega)$ of (5.11a) is

$$(5.12) \quad \mathbf{J} = \begin{pmatrix} -k_1 & k_2x_3 & k_2x_2 \\ k_1 & -k_2x_3 - 2k_3x_2 & -k_2x_2 \\ 0 & 2k_3x_2 & 0 \end{pmatrix}.$$

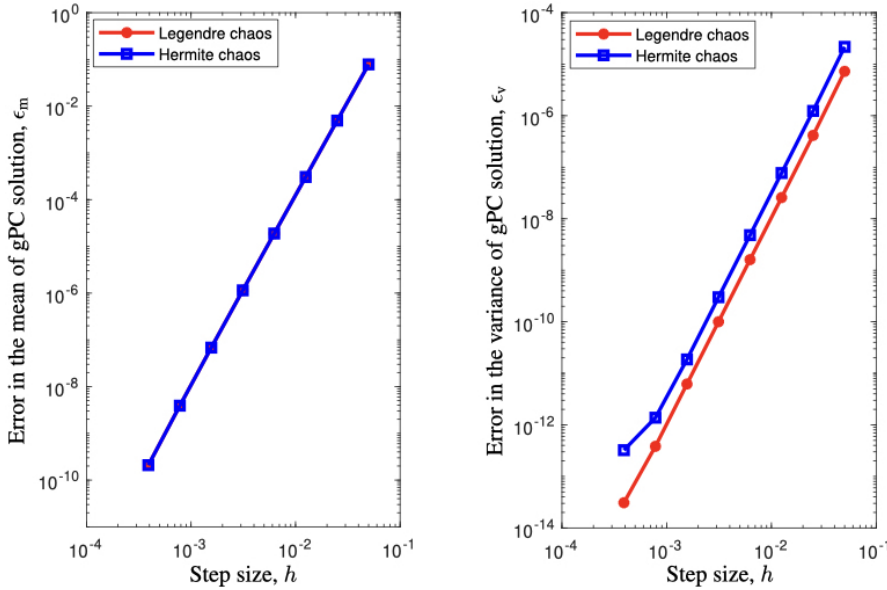


FIG. 5.5. Errors in the mean, ϵ_m , and variance, ϵ_v , of the gPC solution to (5.8) obtained via either Legendre or Hermite chaos of order $P = 3$ with the sixth-order Lobatto IIIB method. These are plotted as function of step size h . The choice of the polynomial type is dictated by the PDF of model inputs ξ .

TABLE 5.5

Empirical convergence orders, p_m and p_v , of the solution to (5.8) obtained via either Legendre or Hermite chaos of order $P = 3$ with the sixth-order Lobatto IIIB method as function of step size h .

Step size h	$\frac{1}{20}$	$\frac{1}{40}$	$\frac{1}{80}$	$\frac{1}{160}$	$\frac{1}{320}$	$\frac{1}{640}$	$\frac{1}{1280}$	$\frac{1}{2560}$
Legendre p_m	4.028	4.020	4.026	4.026	4.041	4.072	4.127	
Legendre p_v	4.237	4.080	3.997	4.086	4.139	4.008	3.832	
Hermite p_m	4.028	4.020	4.026	4.026	4.041	4.072	4.127	
Hermite p_v	4.238	4.080	3.996	4.087	4.136	3.830	2.305	

According to the Chebyshev inequality [20], the element $J_{22} \triangleq -k_2x_3 - 2k_3x_2$ of this matrix satisfies the condition

$$(5.13) \quad \mathbb{P}\{|J_{22} - \mathbb{E}\{J_{22}\}| < 2\sigma\} \geq 1 - \frac{\sigma^2}{4\sigma^2} = \frac{3}{4} \quad \forall t \in [0,1],$$

where $\sigma^2 \triangleq \mathbb{E}\{(J_{22} - \mathbb{E}\{J_{22}\})^2\}$. Hence,

$$(5.14) \quad P\{\mathbb{E}\{J_{22}\} - 2\sigma < J_{22} < \mathbb{E}\{J_{22}\} + 2\sigma\} \geq \frac{3}{4} \quad \forall t \in [0,1].$$

We use Monte Carlo simulations consisting of 1000 realizations of (5.11) solved with the 3-stage Radau IIA scheme—it is A-stable, L-stable, and B-convergent of order 3 [19]—to compute $\mathbb{E}\{J_{22}\}$ and σ . For the uniform or Gaussian $\xi(\omega) = \{\xi_1, \xi_2\}$ and for all $t \in [0, 1]$, this procedure results in

$$(5.15) \quad \text{uniform } \xi: \begin{aligned} -2.835 \times 10^3 &\leq \mathbb{E}\{J_{22}(t)\} \leq -2.062 \times 10^3, \\ -2.904 \times 10^3 &\leq \mathbb{E}\{J_{22}(t)\} - 2\sigma(t) \leq -2.176 \times 10^3, \\ -2.765 \times 10^3 &\leq \mathbb{E}\{J_{22}(t)\} + 2\sigma(t) \leq -1.948 \times 10^3 \end{aligned}$$

or

$$(5.16) \text{ Gaussian } \xi: \begin{aligned} & -2.836 \times 10^3 \leq \mathbb{E}\{J_{22}(t)\} \leq -2.064 \times 10^3, \\ & -2.958 \times 10^3 \leq \mathbb{E}\{J_{22}(t)\} - 2\sigma(t) \leq -2.263 \times 10^3, \\ & -2.714 \times 10^3 \leq \mathbb{E}\{J_{22}(t)\} + 2\sigma(t) \leq -1.864 \times 10^3, \end{aligned}$$

respectively. According to (5.14) and Theorem 4.1 (or Remark 4.2), random ODEs (5.11a) are stiff with probability no less than 3/4. According to Theorem 4.2, the corresponding gPC equations are stiff as well.

For the mutually independent random inputs $\xi_1(\omega)$ and $\xi_2(\omega)$ distributed uniformly on $[-1, 1]$, the mean and variance of the solution to (5.11) obtained via Legendre chaos of the highest order $P = 3$ are shown in Figure 5.6. Given the vast disparity between the rate constants k_1, k_2 , and k_3 , these statistics for the concentrations $x_1(t, \omega)$ and $x_3(t, \omega)$ change with time significantly faster than their counterparts for $x_2(t, \omega)$.

The modified stiffness ratio $\tilde{s}(t)$ and the Lipschitz constant $\|\tilde{\mathbf{J}}(t)\|_1$ of the gPC equations for this problem are plotted in Figure 5.7 for several values of P ; both of these quantities are large, signaling the stiffness of the gPC equations, which is in agreement with the theoretical prediction above. Finally, Figure 5.8 demonstrates that the errors of the solution’s mean and variance decay quickly as P increases, illustrating the effectiveness of the gPC with parallel MIRK methods.

Although not shown here, the results for the normally distributed inputs $\xi_1(\omega)$ and $\xi_2(\omega)$ are qualitatively identical. The modified stiffness ratio $\tilde{s}(t)$ and the Lipschitz constant $\|\tilde{\mathbf{J}}(t)\|_1$ of the Hermite chaos equations are of the same order as their

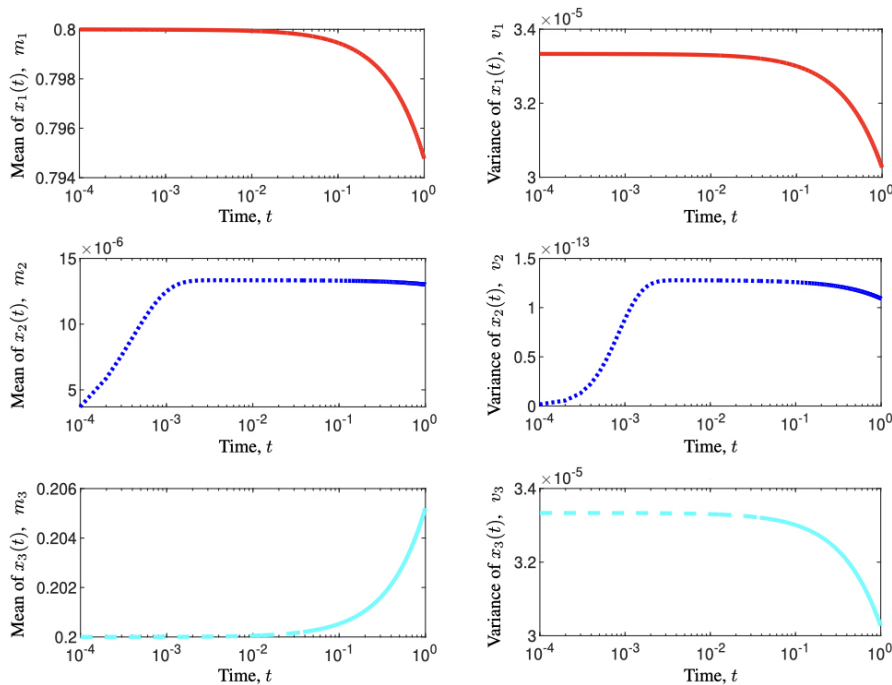


FIG. 5.6. Mean, $m_i(t) \triangleq \mathbb{E}\{\hat{x}_i(t_k, \omega)\}$, and variance, $v_i(t) \triangleq \mathbb{E}\{(\hat{x}_i(t_k, \omega) - m_i)^2\}$, of the solution to (5.11), $\hat{x}_i(t, \omega)$ ($i = 1, 2, 3$), obtained via Legendre chaos of the highest order $P = 3$.

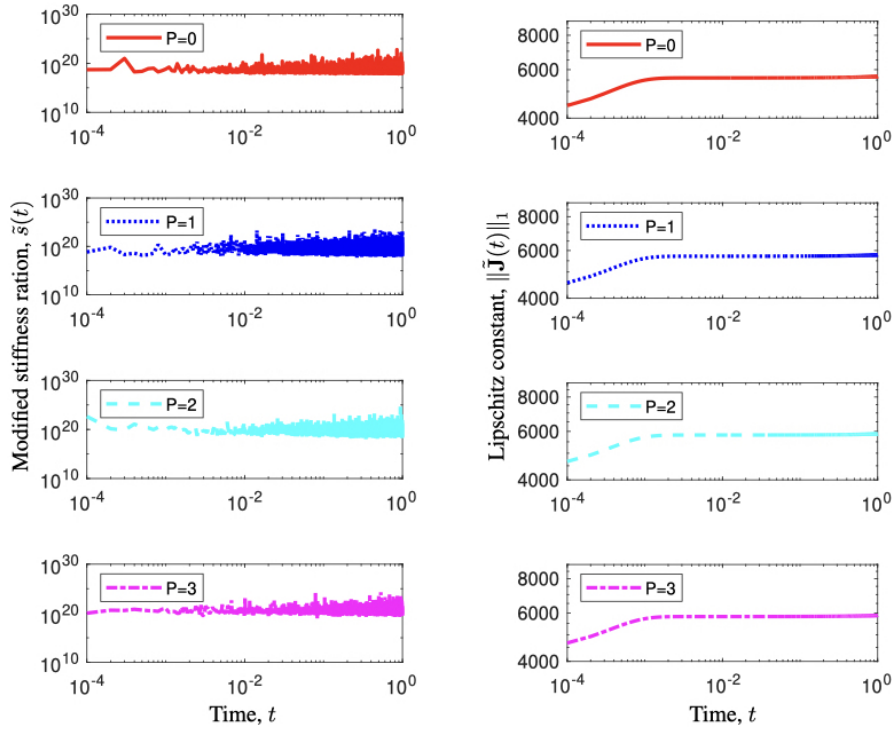


FIG. 5.7. Modified stiffness ratio $\bar{s}(t)$ and the Lipschitz constant $\|\tilde{\mathbf{J}}(t)\|_1$ of the gPC equations for problem (5.11) with uniformly distributed ξ . The results are shown for several values of the highest order of Legendre chaos, P .

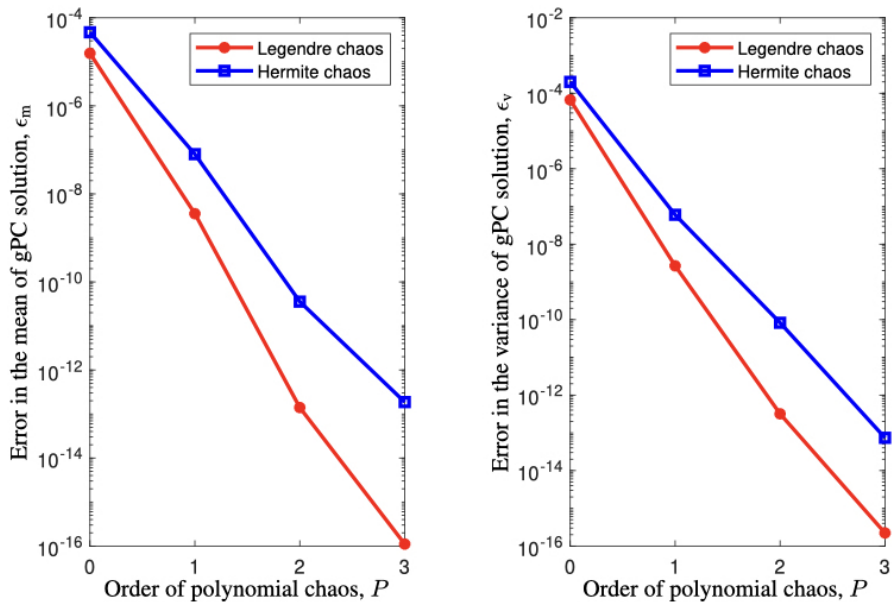


FIG. 5.8. Errors of the mean, ϵ_m , and variance, ϵ_v , of the gPC solution to (5.11) as function of the highest order of Legendre or Hermite chaos, P . The choice of the polynomial type is dictated by the PDF of model inputs ξ .

counterparts in Figure 5.7. The errors ϵ_m and ϵ_v decay appreciably faster with P than they do in the case of Legendre chaos (Figure 5.8).

5.4. ODEs from discretized parabolic equations. Finally, we consider a state variable $u(x, t, \omega)$, whose spatiotemporal evolution is described by a parabolic (diffusion) equation,

$$(5.17a) \quad \frac{\partial u}{\partial t} - \frac{\partial^2 u}{\partial x^2} = q(x, t, \omega), \quad 0 < x < 1, \quad 0 < t \leq 1,$$

subject to initial and boundary conditions

$$(5.17b) \quad u(x, 0, \omega) = 0, \quad u(0, t, \omega) = u(1, t, \omega) = 0.$$

The random source term $q(x, t, \omega)$ has the form

$$(5.18) \quad q(x, t, \omega) = x(1-x) + e^{1+\sigma\gamma(t,\omega)}, \quad \gamma(t, \omega) = \frac{1}{\pi^2} \sum_{n=1}^N \frac{1}{n^2} \sin(2\pi nt)\xi_n(\omega),$$

where $\boldsymbol{\xi}(\omega) \triangleq (\xi_1, \dots, \xi_N)^\top$ is a vector of mutually independent random variables, each of which is either uniformly distributed on $[-1, 1]$ or standard Gaussian. The series in (5.18) can be viewed as a truncated (after N terms) Karhunen–Loève expansion of the random process $\gamma(t, \omega)$ whose covariance function has eigenvalues $1/(2\pi^4 n^4)$ [42].

Solving (5.17) with the method of lines [7, 38, 31]—e.g., via the central finite-difference discretization of the spatial derivatives on a uniform grid with mesh size $\Delta x = 1/(m+1)$, where m is a positive integer—gives rise to a system of random ODEs,

$$(5.19) \quad \begin{cases} \frac{d\mathbf{U}}{dt} = \mathbf{B} \cdot \mathbf{U} + \mathbf{Q}, & t \in (0, 1], \\ \mathbf{U}(0) = \mathbf{0}, \end{cases}$$

where $\mathbf{U} \in \mathbb{R}^m$, \mathbf{B} is a tridiagonal matrix

$$(5.20) \quad \mathbf{B} = \frac{1}{(\Delta x)^2} \begin{pmatrix} -2 & 1 & & & \\ 1 & -2 & 1 & & \\ & \ddots & \ddots & \ddots & \\ & & 1 & -2 & 1 \\ & & & 1 & -2 \end{pmatrix}_{m \times m},$$

and the vector $\mathbf{Q} = (Q_1, \dots, Q_m)^\top$ has components

$$(5.21) \quad Q_k = x_k(1-x_k) + \exp \left\{ 1 + \frac{\sigma}{\pi^2} \sum_{n=1}^N \frac{1}{n^2} \sin(2\pi nt)\xi_n \right\}, \quad 1 \leq k \leq m.$$

For any $\omega \in \Omega$, the Jacobian of (5.19) is $\mathbf{J} = \mathbf{B}$. Its eigenvalues are [7]

$$(5.22) \quad \lambda_k = -\frac{2}{(\Delta x)^2} \left[1 + \cos \left(\frac{k\pi}{m+1} \right) \right], \quad 1 \leq k \leq m.$$

It follows from (5.22) that the stiffness ratio is

$$(5.23) \quad \bar{s}(t) = \frac{\max_k \{|\lambda_k|\}}{\min_k \{|\lambda_k|\}} \approx \frac{4m^2}{\pi^2} \quad \text{if } m \text{ is large.}$$

According to Definition 2.6, (5.19) with large m is a system of stiff random ODEs.

Our stiffness analysis in section 4 confirms this result. Indeed, the element J_{11} of the Jacobian matrix \mathbf{J} in (5.19) is

$$(5.24) \quad J_{11} = -\frac{2}{(\Delta x)^2} = -2(m+1)^2.$$

Hence, for large m , $|J_{11}|$ is sufficiently large with probability 1. According to Theorem 4.1 (or Remark 4.2 or Corollary 4.1), random ODEs (5.19) with large m are stiff with probability 1. According to Theorem 4.2 (or Corollary 4.1), the corresponding gPC equations are stiff as well.

The derivations similar to those for $\bar{s}(t)$ in (5.23) yield the modified stiffness ratio for the gPC equations (3.8),

$$(5.25) \quad \tilde{s}(t) \approx \frac{4m^2}{\pi^2} \quad \text{for large } m,$$

and the Lipschitz constant,

$$(5.26) \quad \|\tilde{\mathbf{J}}(t)\|_1 = \frac{4}{(\Delta x)^2} = 4(m+1)^2.$$

For large m , $\tilde{s}(t)$ and $\|\tilde{\mathbf{J}}(t)\|_1$ are large, which implies that the gPC equations are stiff, in agreement with the theoretic considerations above. These results hold for both uniform and Gaussian distributions of the random variables $\boldsymbol{\xi}$ and for both Legendre and Hermite chaos expansions of the highest order $P = 0, 1, 2$, or 3 .

The theoretical considerations reported in Appendix A reveal that error of the mean of the gPC solution to (5.19), ϵ_m , is independent of P and depends on the accuracy of the numerical scheme employed. Error of the variance of the gPC solution to (5.19), ϵ_v , is displayed in Figure 5.9. It demonstrates an exponential convergence rate, illustrating the effectiveness of the gPC with parallel MIRK methods. In these calculations, we used $\Delta x = 0.02$ and $N = 10$ random variables $\boldsymbol{\xi}$ and employed the gPC solution of the highest order $P = 4$ as the ground truth.

6. Summary. Stiff equations are ubiquitous in scientific computing. In the deterministic setting, considerable advancements have been made in their analysis and numerical treatment; similar studies of stiff random equations are scarce. We fill this void by analyzing the gPC with parallel MIRK methods as a means of solving stiff random ODEs.

The lack of literature on stiff random ODEs gave us impetus to generalize some pragmatic definitions of stiffness of deterministic equations to the random setting. We posit that this resulted in several reasonable and computable mathematical descriptions of stiff random ODEs.

We presented a general framework for solving stiff random ODEs (1.1) via the gPC with parallel MIRK methods. Our study demonstrates the importance of stiffness analysis in stochastic problems and illustrates the advantages of the parallel MIRK schemes.

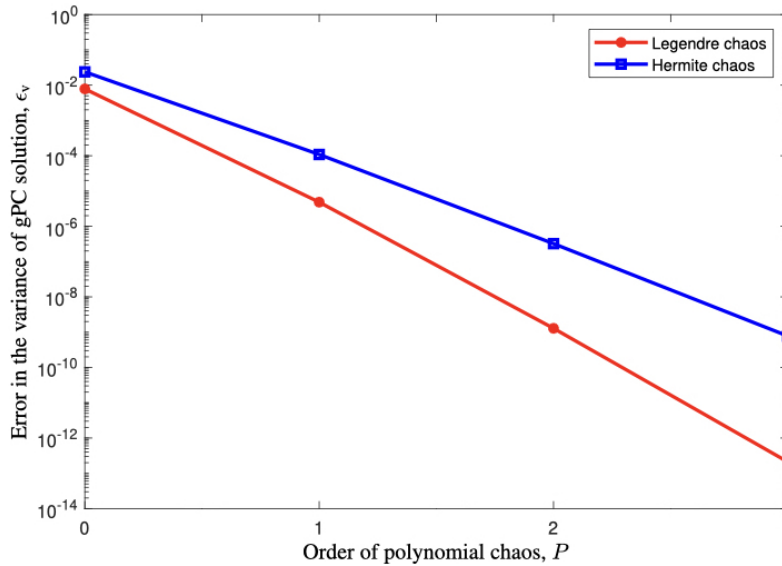


FIG. 5.9. Error in variance, ϵ_v , of the gPC solution to (5.19) as function of the highest order of Legendre or Hermite chaos, P . The choice of the polynomial type is dictated by the PDF of model inputs ξ .

We introduced a series of workable strategies for an a priori identification of random ODEs as stiff. We also identified a connection between the Jacobian matrices of the random ODEs (1.1) and the resulting gPC equations (3.8). Exploiting this connection, we established a direct computable way to determine whether these gPC equations are stiff. This theoretical analysis is relevant to numerical treatment of random ODEs and PDEs by methods other than gPC, e.g., by Monte Carlo simulations, stochastic collocation on sparse grids, etc.

We presented four numerical experiments, dealing with systems of random ODEs and a spatially discretized PDE. These numerical results confirm our theoretical analysis of stiffness and serve to establish gPC with the parallel MIRK methods as a feasible and effective tool for their solution. They also demonstrate the limitations of the standard high-order techniques, such as the fourth-order RK method and the sixth-order Lobatto IIIB method, in this random setting.

More work remains to be done on the development of efficient methods for solving stiff systems with random coefficients. While our study focused on the impact of stiffness on the performance of gPC, this issue is relevant for multilevel Monte Carlo and stochastic collocation on sparse grids. Another area of future research is the deployment of parallel MIRK schemes on advanced computer architectures in order to alleviate the curse of dimensionality, especially for stiff problems. Finally, the development of dedicated numerical methods for stiff systems with random coefficients remains an open challenge.

Appendix A. Error measure for mean gPC solution to linear ODEs.

Consider linear ODEs of the form

$$(A.1) \quad \begin{cases} \frac{d\mathbf{U}}{dt} = \mathbf{A} \cdot \mathbf{U} + \mathbf{Q}, & t > 0, \\ \mathbf{U}(0) = \mathbf{0}, \end{cases}$$

where \mathbf{A} is a constant matrix and \mathbf{Q} is a function of N random variables $\boldsymbol{\xi}(\omega) \triangleq (\xi_1, \dots, \xi_N)^\top$. Its gPC solution, truncated after M terms, is written as

$$(A.2) \quad \mathbf{U}_{\text{gPC}}(t, \omega) = \sum_{k=1}^M \mathbf{U}_k(t) \Psi_k(\boldsymbol{\xi}),$$

where the deterministic vector-functions $\{\mathbf{U}_k(t)\}$ are obtained from the corresponding gPC equations (3.7). The ensemble mean of the gPC solution is

$$(A.3) \quad \mathbb{E}\{\mathbf{U}_{\text{gPC}}\} = \mathbf{U}_1(t),$$

where $\mathbf{U}_1(t)$ is a solution of

$$(A.4) \quad \begin{cases} \frac{d\mathbf{U}_1}{dt} = \mathbf{A} \cdot \mathbf{U}_1 + \mathbb{E}\{\mathbf{Q}\}, & t > 0, \\ \mathbf{U}_1(0) = \mathbf{0}. \end{cases}$$

This solution \mathbf{U}_1 is independent of the highest order of gPC. Thus, the error measure ϵ_m is independent of the highest order of gPC; it is affected by the accuracy of the numerical scheme employed to solve (A.4).

Acknowledgments. The authors thank the two anonymous reviewers whose suggestions have helped us improve the original version of this manuscript.

REFERENCES

- [1] R. C. AIKEN, *Stiff Computation*, Oxford University Press, Oxford, 1985.
- [2] A. ALEXANDERIAN, O. P. LE MAÎTRE, H. N. NAJM, M. ISKANDARANI, AND O. M. KNIO, *Multiscale stochastic preconditioners in non-intrusive spectral projection*, J. Sci. Comput., 50 (2012), pp. 306–340.
- [3] I. BABUŠKA, F. NOBILE, AND R. TEMPONE, *A stochastic collocation method for elliptic partial differential equations with random input data*, SIAM J. Num. Anal., 45 (2007), pp. 1005–1034.
- [4] D. A. BARAJAS-SOLANO AND D. M. TARTAKOVSKY, *Stochastic collocation methods for nonlinear parabolic equations with random coefficients*, SIAM/ASA J. Uncertain. Quantif., 4 (2016), pp. 475–494, <https://doi.org/10.1137/130930108>.
- [5] P. BONNAIRE, P. PETTERSSON, AND C. F. SILVA, *Intrusive generalized polynomial chaos with asynchronous time integration for the solution of the unsteady Navier–Stokes equation*, Comput. Fluids, 223 (2021), 104952.
- [6] K. BURRAGE, F. H. CHIPMAN, AND P. H. MUIR, *Order results for mono-implicit Runge–Kutta methods*, SIAM J. Numer. Anal., 31 (1994), pp. 876–891.
- [7] G. D. BYRNE AND A. C. HINDMARSH, *Stiff ODE solvers: A review of current and coming attractions*, J. Comput. Phys., 70 (1987), pp. 1–62.
- [8] J. R. CASH AND A. SINGHAL, *Mono-implicit Runge–Kutta formulae for the numerical integration of stiff differential systems*, IMA J. Numer. Anal., 2 (1982), pp. 211–227.
- [9] C. W. CRYER, *A new class of highly-stable methods: A_0 -stable methods*, BIT Numer. Math., 13 (1973), pp. 153–159.
- [10] C. F. CURTISS AND J. O. HIRSCHFELDER, *Integration of stiff equations*, Proc. Natl. Acad. Sci. USA, 38 (1952), pp. 235–243.
- [11] G. G. DAHLQUIST, *A special stability problem for linear multistep methods*, BIT Numer. Math., 3 (1963), pp. 27–43.
- [12] B. N. L. EHLE, *On Padé Approximations to the Exponential Function and A-stable Methods for the Numerical Solution of Initial Value Problems*, Ph.D. thesis, University of Waterloo Waterloo, Ontario, Canada, 1969.
- [13] G. S. FISHMAN, *Monte Carlo: Concepts, Algorithms, and Applications*, Springer-Verlag, Berlin, 2013.
- [14] R. FRANK, J. SCHNEID, AND C. W. UEBERHUBER, *The concept of B-convergence*, SIAM J. Numer. Anal., 18 (1981), pp. 753–780.

- [15] R. FRANK, J. SCHNEID, AND C. W. UEBERHUBER, *Order results for implicit Runge–Kutta methods applied to stiff systems*, SIAM J. Numer. Anal., 22 (1985), pp. 515–534.
- [16] M. GERRITSMAN, J.-B. VAN DER STEEN, P. VOS, AND G. KARNIADAKIS, *Time-dependent generalized polynomial chaos*, J. Comput. Phys., 229 (2010), pp. 8333–8363.
- [17] R. G. GHANEM AND P. D. SPANOS, *Stochastic Finite Elements: A Spectral Approach*, Dover, Mineola, NY, 2003.
- [18] E. HAIRER, S. NØRSETT, AND G. WANNER, *Solving Ordinary Differential Equations I: Nonstiff Problems*, Springer-Verlag, Berlin, 1987.
- [19] E. HAIRER AND G. WANNER, *Solving Ordinary Differential Equations II: Stiff and Differential Algebraic Problems*, 2nd ed., Springer-Verlag, Berlin, 1996.
- [20] O. KALLENBERG, *Foundations of Modern Probability*, Springer-Verlag, Berlin, 2002.
- [21] J. D. LAMBERT, *Numerical Methods for Ordinary Differential Systems: The Initial Value Problem*, John Wiley & Sons, New York, 1991.
- [22] R. J. LEVEQUE, *Finite Difference Methods for Ordinary and Partial Differential Equations: Steady-State and Time-Dependent Problems*, SIAM, Philadelphia, 2007.
- [23] O. P. L. MAÎTRE, L. MATHELIN, O. M. KNIO, AND M. Y. HUSSAINI, *Asynchronous time integration for polynomial chaos expansion of uncertain periodic dynamics*, Discrete Contin. Dyn. Syst. Ser. A, 28 (2010), pp. 199–226.
- [24] T. E. MALTBA, H. ZHAO, AND D. M. TARTAKOVSKY, *Autonomous learning of nonlocal stochastic neuron dynamics*, J. Cogn. Neurodyn., (2021), <https://doi.org/10.1007/s11571-021-09731-9>.
- [25] P. H. MUIR AND W. H. ENRIGHT, *Relationships among some classes of IRK methods and their stability functions*, BIT Numer. Math., 27 (1987), pp. 403–423.
- [26] E. MUSHARBASH, F. NOBILE, AND E. VIDLIČKOVÁ, *Symplectic dynamical low rank approximation of wave equations with random parameters*, BIT Numer. Math., 60 (2020), pp. 1153–1201.
- [27] A. NARAYAN AND T. ZHOU, *Stochastic collocation on unstructured multivariate meshes*, Comm. Comput. Phys, 18 (2015), pp. 1–36.
- [28] A. PROTHERO AND A. ROBINSON, *On the stability and accuracy of one-step methods for solving stiff systems of ordinary differential equations*, Math. Comput., 28 (1974), pp. 145–162.
- [29] A. QUARTERONI, R. SACCO, AND F. SALERI, *Numerical Mathematics*, 2nd ed., Vol. 37, Springer-Verlag, Berlin, 2007.
- [30] H. H. ROBERTSON, *The solution of a set of reaction rate equations*, in Numerical Analysis: An Introduction, J. Walsh, ed., Academic Press, London, 1966, pp. 178–182.
- [31] L. F. SHAMPINE AND C. W. GEAR, *A user’s view of solving stiff ordinary differential equation*, SIAM Rev., 21 (1979), pp. 1–17.
- [32] W. SHI AND C. ZHANG, *Error analysis of generalized polynomial chaos for nonlinear random ordinary differential equations*, Appl. Numer. Math., 62 (2012), pp. 1954–1964.
- [33] W. SHI AND C. ZHANG, *Generalized polynomial chaos for nonlinear random delay differential equations*, Appl. Numer. Math., 115 (2017), pp. 16–31.
- [34] T. TANG AND T. ZHOU, *Recent developments in high order numerical methods for uncertainty quantification*, Sci. Sin. Math., 45 (2015), pp. 891–928.
- [35] K. UM, E. J. HALL, M. A. KATSOLAKIS, AND D. M. TARTAKOVSKY, *Causality and Bayesian Network PDEs for multiscale representations of porous media*, J. Comput. Phys., 394 (2019), pp. 658–678, <https://doi.org/10.1016/j.jcp.2019.06.007>.
- [36] D. A. VOSS, *Parallel Mono-Implicit Runge–Kutta Methods for Stiff ODEs*, report, Western Illinois University, 1995.
- [37] D. A. VOSS, *Parallel MIRK methods for ODEs*, CWI Quart., 11 (1998), pp. 101–111.
- [38] D. A. VOSS AND P. H. MUIR, *Mono-implicit Runge–Kutta schemes for the parallel solution of initial value ODEs*, J. Comput. Appl. Math., 102 (1999), pp. 235–252.
- [39] P. WANG, A. M. TARTAKOVSKY, AND D. M. TARTAKOVSKY, *Probability density function method for Langevin equations with colored noise*, Phys. Rev. Lett., 110 (2013), 140602.
- [40] O. B. WIDLUND, *A note on unconditionally stable linear multistep methods*, BIT Numer. Math., 7 (1967), pp. 65–70.
- [41] D. XIU, *Numerical Methods for Stochastic Computations: A Spectral Method Approach*, Princeton University Press, Princeton, NJ, 2010.
- [42] D. XIU AND J. S. HESTHAVEN, *High-order collocation methods for differential equations with random inputs*, SIAM J. Sci. Comput., 27 (2005), pp. 1118–1139.